

# Charge Transfer Across the Nanocrystalline-DNA Interface: Probing DNA Recognition

Tijana Rajh,<sup>\*,†</sup> Zoran Saponjic,<sup>†</sup> Jianqin Liu,<sup>†</sup> Nada M. Dimitrijevic,<sup>†</sup> Norbert F. Scherer,<sup>§</sup> Manuel Vega-Arroyo,<sup>†</sup> Peter Zapol,<sup>†,‡</sup> Larry A. Curtiss,<sup>†,‡</sup> and Marion C. Thurnauer<sup>†</sup>

*Chemistry Division, Materials Science Division, Argonne National Laboratory, Argonne, Illinois 60439, and Department of Chemistry, University of Chicago, Chicago, Illinois 60637*

*Received February 26, 2004; Revised Manuscript Received March 26, 2004*

## ABSTRACT

Hybrid nanocomposites that electronically link TiO<sub>2</sub> nanoparticles to DNA oligonucleotides were developed. The linking of biomolecules with inorganic components was achieved by using bridging enediol ligands, such as dopamine (DA), which facilitate hole transfer across the interface, establishing efficient crosstalk between the biomolecule and metal oxide nanoparticles. The inherent programmability of oligonucleotides builds recognition properties into the hybrid system, allowing selective binding of nanoparticles to targeted molecules. The inorganic nanoparticles are inherently photoresponsive and therefore serve as a source of photogenerated charges that act as reporters of the electronic properties of the biomolecules. These photoactive bioinorganic TiO<sub>2</sub>/DA/DNA triads are capable of complex photo chemistries such as light induced manipulation of biomolecules and their switching functions. Consequently, light induced extended charge separation in these systems was found to be a fingerprint of DNA oligonucleotide hybridization.

Molecular recognition of biomolecules and their site selective bindings are topics of significant interest because of unique applications in the fields of patterning, genome sequencing and drug affinity studies.<sup>1</sup> DNA oligonucleotides hold a special promise because of the exquisite programmability of the nucleic-acid-based recognition system. Investigation of oligonucleotide hybridization mechanisms has mainly focused on optical detection using fluorescence-labeled oligonucleotides with dyes<sup>2</sup> or quantum dots<sup>3</sup> and enhanced absorption of light by oligonucleotide-modified gold nanoparticles.<sup>4</sup> Although control of the spatial position on the nanoscale is a necessary step for molecular recognition, it is not sufficient for exploiting the full potential that DNA can play in bioelectronics. It is desirable that after positioning of an inert biomolecule with biological specificity an activated process changes the biomolecule's redox state and selectively catalyzes a string of consecutive responses.<sup>5</sup> This opens up the possibility of the electronic transduction of DNA sequence and hybridization, as well as development of new electrochemical probes for DNA-binding proteins, both of which are major challenges in bioelectronics. The advantage of this approach is sensitive, direct detection of

oligonucleotide sequence, mismatches, and interactions of DNA with DNA-binding proteins.<sup>6</sup>

Nanocrystalline metal oxide semiconductor particles are photoactive and act as miniaturized photoelectrochemical cells. However, their reactivity will depend on the redox properties of the molecules that are attached to the nanoparticle surface. Recently we have reported that TiO<sub>2</sub> nanoparticles (~50 Å) having appropriate surface modification bind DNA oligonucleotides and retain the ability to hybridize with the complementary DNA.<sup>7</sup> Herein we report that absorption of light in these TiO<sub>2</sub>/oligonucleotide nanocomposites leads to instantaneous charge separation across the nanoparticle interface followed by efficient hole scavenging in double-stranded DNA but not single-stranded DNA. Moreover, we observed different abilities for scavenging photogenerated holes in the system containing mismatched DNA oligonucleotides compared to fully matched DNA. The initial charge separation sequence in these hybrid bioinorganic nanocomposites was found to be analogous to the reaction mechanisms in supramolecular triads, capable of performing redox functions at the nanoscale level, depending on the thermodynamic properties of the triad constituents<sup>8,9</sup> (Figure 1). Additionally, the DNA oligonucleotides linked to the nanoparticle provide, through sequence design, binding specificity to selected substrates. This forms a basis for a

\* Corresponding author.

<sup>†</sup> Chemistry Division, Argonne National Laboratory.

<sup>‡</sup> Materials Science Division, Argonne National Laboratory.

<sup>§</sup> University of Chicago.

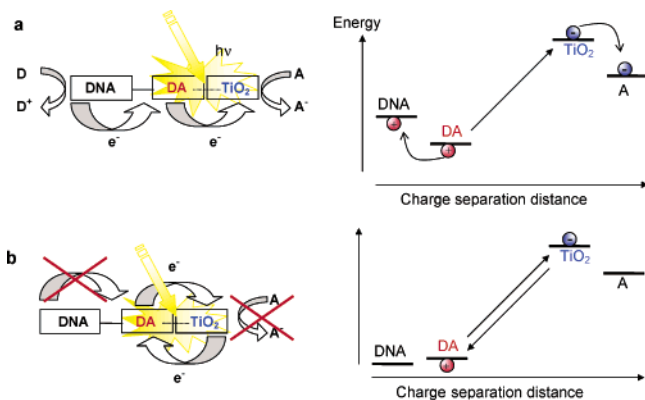


**Figure 1.** Salient features of charge separation process in hybrid  $\text{TiO}_2$ /oligonucleotide nanocomposites. Electron transfer in hybrid bioinorganic triad systems provides the foundation to investigate how DNA redox reactions are coupled to the initial photoinduced charge separation in  $\text{TiO}_2$ /dopamine. For example, when redox properties of attached DNA are more negative than the oxidation potential of  $\text{TiO}_2$ /dopamine (a), the photogenerated holes are transferred to attached DNA. Light induced charge separation in this system extends to distances at which charge recombination does not occur. Photogenerated charges can subsequently participate in redox reactions with electron-accepting (A) and electron-donating (D) redox couples present in the nanocomposite environment. However, when the oxidation potential of attached DNA oligonucleotides is more positive than the potential of photogenerated holes in the  $\text{TiO}_2$ /DA system (b), sequential charge separation does not occur and photogenerated charge pairs recombine with no net chemical reaction.

completely new family of DNA-based site selective electrochemical nanomachines capable of photosensing, photo-switching, and/or site selective photocatalysis that operate on the principles of DNA-mediated photoinduced charge separation in nanocrystalline semiconductors.

Titanium dioxide is a photocatalytic material, which has been extensively studied because it is inexpensive, nontoxic, and photostable.<sup>10</sup> Absorption of light with energy greater than the band gap (3.2 eV) of  $\text{TiO}_2$  particles results in the formation of electron/hole pairs. The photogenerated carriers migrate to the semiconductor/solution interface where they can oxidize/reduce redox species in solution. Recently we have reported enhanced, reversible, light initiated charge separation and improved optical properties of  $\text{TiO}_2$  after chemical engineering of the nanocrystal surface with different enediol chelating ligands, such as dopamine (DA).<sup>11,12</sup> The coordination sphere of the surface metal atoms in  $\text{TiO}_2$  nanoparticles that are smaller than 200 Å is incomplete and thus exhibits high affinity for oxygen-containing ligands.<sup>11</sup> Oxygen-rich enediol ligands, such as dopamine, form strongly coupled conjugated structures with surface Ti atoms by repairing undercoordination of the surface. As a consequence, the intrinsic properties of a semiconductor change and new hybrid molecular orbitals are generated by a mixing of the orbitals of chelating ligands and the continuum states of metal oxides. Absorption of light by these systems results in excitation of an electron from the chelating ligands directly into the conduction band of the  $\text{TiO}_2$  particle, without transitioning through the enediol excited state. An important

feature of these hybrid systems is that localized orbitals of surface-attached ligands are electronically coupled with the delocalized conduction band of the metal oxide semiconductor. This electronic coupling adds an important asset that charge pairs are instantaneously separated into two phases, the holes localized on the donating organic modifier and the electrons delocalized in the conduction band of  $\text{TiO}_2$ .<sup>13</sup> These features designate the ligands as *conductive leads* that allow electronic wiring of the nanoparticles. When covalently linked (wired) to electron donating moieties, photoinduced electron transfer extends further, ultimately leading to stabilized charge separation, analogous to the charge separation in supramolecular triads.<sup>8,9</sup> Extended charge separation can be detected electronically or can be used for driving electrochemical reactions with surrounding redox species (Figure 1).

Nucleosides of DNA oligonucleotides have redox potentials in a range that allows their oxidation by photogenerated holes in the valence band of  $\text{TiO}_2$ .<sup>14</sup> Guanosine has the lowest oxidation potential and can reduce any of the oxidized bases. Indeed, Warner et al.<sup>15</sup> found that guanine undergoes photooxidative damage in DNA physisorbed on  $\text{TiO}_2$  particles, resulting in the hydroxylation of guanine. Serpone et al.<sup>16</sup> have found that  $\text{TiO}_2$  particles catalyze DNA damage in vitro or in cells. We found that oxidation of nucleobases physisorbed at the surface of 45 Å  $\text{TiO}_2$  particles was accompanied by accumulation of photogenerated electrons in  $\text{TiO}_2$  that is reflected by a broad optical absorption at 700 nm, characteristic of Ti(III) species in  $\text{TiO}_2$ . Accordingly, we determined that thymidine is the only nucleotide that is not oxidized upon photoactivation of  $\text{TiO}_2$  while the yield of oxidation of the remaining three bases is: cytidine < adenosine  $\approx$  guanosine. The result that thymidine is not oxidized by  $\text{TiO}_2$  particles is consistent with the observation that photogenerated holes in nanocrystalline  $\text{TiO}_2$  particles lose significant energy upon trapping as oxygen-centered radicals on the surface. The energy of the surface-trapped holes is in the range  $1.6 \text{ V} \leq \equiv \text{TiO}^{\bullet}, \text{H}^+ / \equiv \text{TiOH} \leq 1.7 \text{ V}$  vs. NHE,<sup>17</sup> which is insufficient for oxidation of thymidine.

Oligonucleotides with different nucleotide sequences were coupled to metal oxide semiconductor particles through a dopamine linker.<sup>18</sup> We have demonstrated dopamine-induced restructuring of the Ti surface atoms, allowing for irreversible binding of dopamine molecules to the nanoparticle surface.<sup>11</sup> Therefore, the amino group of dopamine was linked to the specific single strands of oligonucleotides (16–20 nucleotides long) having carboxyl groups at the 5' end (via the intermediate *N*-hydroxy-succinimide ester)<sup>19,20</sup> and subsequently linked to the surface of  $\text{TiO}_2$  nanoparticles. Dopamine-terminated DNA oligonucleotides (DA-DNA) show the same high affinity to bind undercoordinated surface atoms as dopamine molecules themselves. Therefore, after mixing DA-DNA with  $\text{TiO}_2$  nanoparticles visible absorption of the  $\text{TiO}_2$ /DA charge-transfer complex is observed. The number of oligonucleotides bound to each particle was determined from the change in the optical absorption after binding (inset, Figure 2). Typically, the change in the absorption after binding was consistent with having between 2 and 3

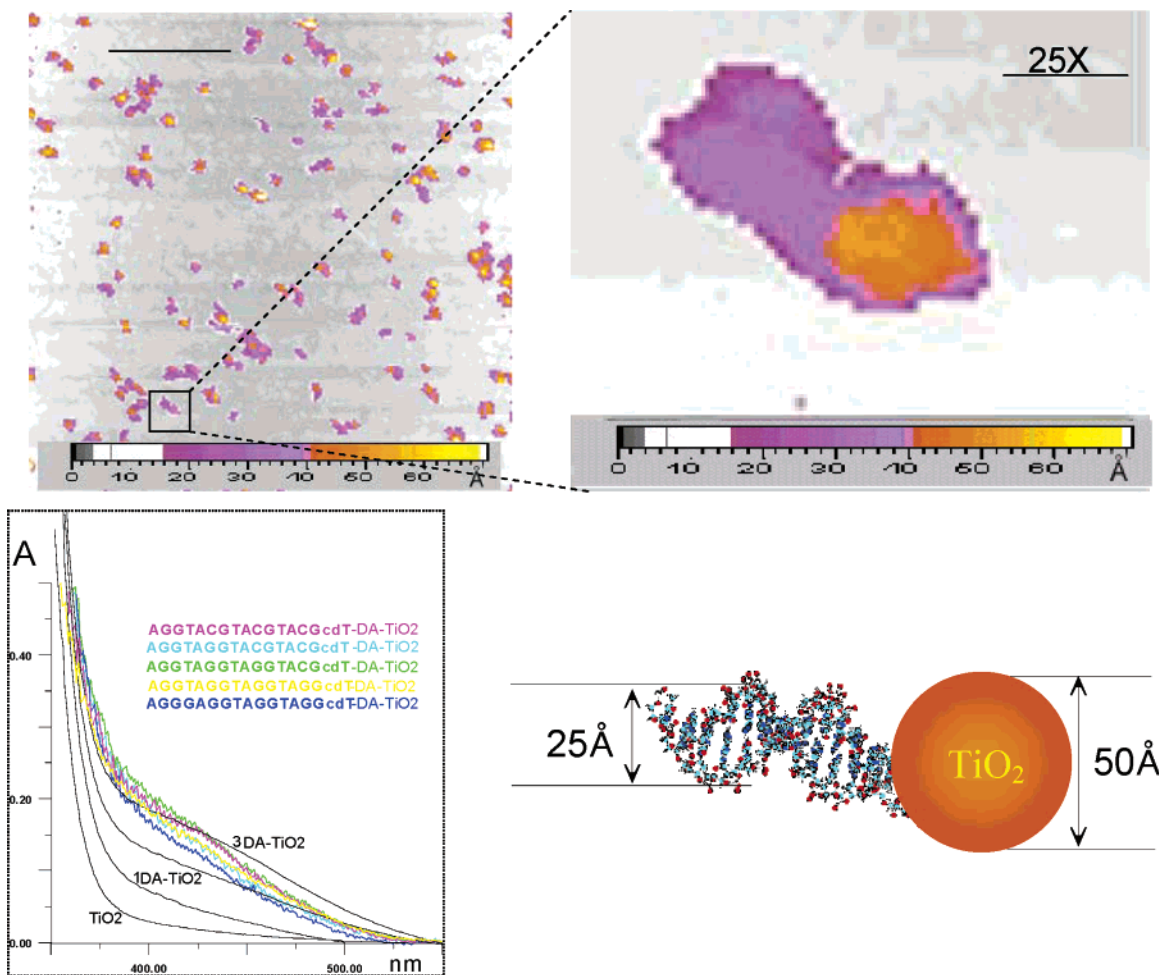


**Figure 2.** AFM image of 50 Å  $\text{TiO}_2$  nanoparticles linked to 16-base pair double-stranded oligonucleotides (Digital Instruments, Bioscope). The samples were prepared in 40 mM phosphate buffer according to the procedure described elsewhere<sup>7</sup> and spin coated onto the freshly cleaved mica substrate. While the two images have different in-plane scale, the height scale is the same for both images. The color-coded scale of the sample heights is presented on the bottom of each image while the in-plane scale is indicated with the bar on the image. A model of  $\text{TiO}_2$  nanoparticles linked to 16-base pair double-stranded DNA is depicted in the bottom right corner. The inset on the bottom left corner presents the absorption spectra of  $\text{TiO}_2$  nanoparticles linked to: none, one, two, and three dopamine molecules per particle (black); and different 16-base pair oligonucleotides end-labeled with dopamine molecules (color) used for obtaining AFM images.

oligonucleotides per particle. Oligonucleotide-modified particles were then hybridized with complementary DNA strands of the same lengths. The image of  $\text{TiO}_2$  particles linked to short oligonucleotides (16 base pairs) was obtained with atomic force microscopy (AFM) (Figure 2). The size of the  $\text{TiO}_2$  nanoparticle in these experiments was 50 Å, comparable in size to the oligonucleotide length (40 Å) (see depicted model, Figure 2). The color-coded height profile of the composites clearly shows that composites contain two parts, one with the height of  $\sim 25$  Å (purple), comparable with the thickness of the DNA oligonucleotide, and the other of 48 Å (orange), comparable to the  $\text{TiO}_2$  diameter, indicating tentacle binding of DNA, which does not wrap around the nanoparticle. The height histogram (not shown) exhibits two maxima, one with the size centered around  $\sim 28$  Å and the other centered around  $\sim 48$  Å. The surface area ratio under the deconvoluted curves in the histogram obtained with AFM imaging presents the average number of oligonucleotides per  $\text{TiO}_2$  particle (between 2 and 3 throughout this work).

The role of sequential electron transfer, and electrochemical parameters, and how they affect the distance dependent

charge separation properties in the oligonucleotide-modified  $\text{TiO}_2$  system was examined with electron paramagnetic resonance (EPR) spectroscopy. While transient optical spectroscopy is a powerful technique for studies of the dynamics of charge transfer in DNA,<sup>21,22</sup> EPR spectroscopy provides an unambiguous identification of the species involved in the charge separation processes by revealing changes in local symmetry and hyperfine couplings along the pathway of charge carriers.<sup>23,24</sup>

Initially, we have identified the radical species formed by photoexcitation of the charge-transfer complex of  $\text{TiO}_2$  nanoparticles with dopamine alone at low temperature (10 K).<sup>25</sup> EPR signals attributed to the reduced electron acceptor ( $\text{Ti}^{3+}$ ) and the oxidized electron donor (dopamine<sup>+</sup>) were obtained. The former weak signal ( $g_{\perp} = 1.988$ ,  $g_{\parallel} = 1.958$ ) is characteristic of a radical in which the unpaired electron occupies the d orbitals of the anatase lattice Ti atoms.<sup>26</sup> The latter EPR signal was observed at  $g = 2.004$ , having a line width of  $\Delta H_{pp} = 16$  G. We attribute this signal to dopamine because the signal narrowed to  $\Delta H_{pp} = 10$  G upon deuteration of dopamine (ring  $\text{D}_2$  or 2,2  $\text{D}_2$ ), indicating the existence

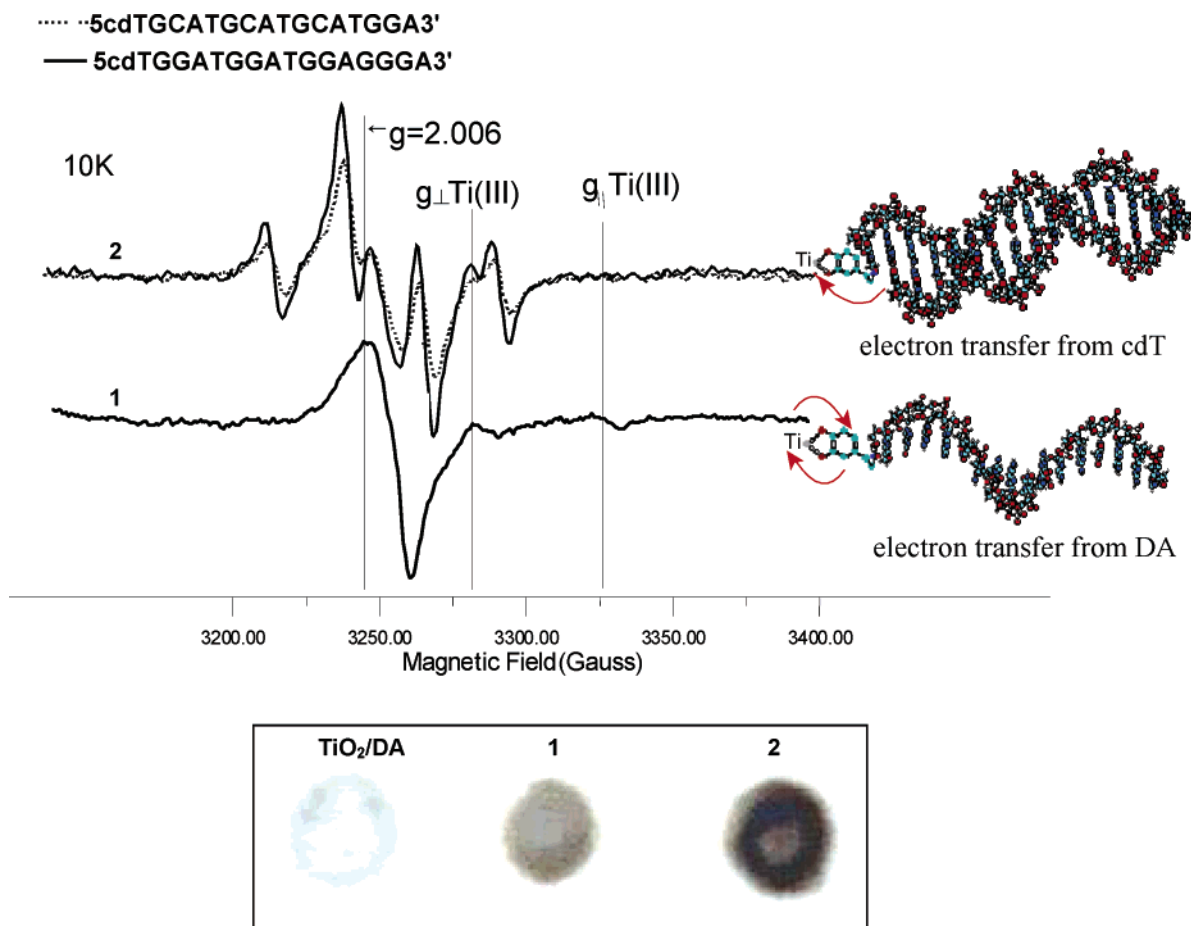


**Figure 3.** Charge separation in 50 Å  $\text{TiO}_2$  particles coupled to 16-base pair single-stranded (1) and double-stranded oligonucleotides (two different sequences) (2). Top: EPR spectra. The samples were illuminated using a Xe 300 W lamp (ILC Corp.), and the spectra recorded at 10 K. EPR setup was described elsewhere.<sup>25</sup> Samples were checked for background EPR signals before irradiation. EPR spectra were recorded with 6.3 G modulation amplitude, 0.1 s time constant, 1 mW microwave power. Bottom: Photoreduction of silver ions under ambient conditions.  $\text{TiO}_2$  nanoparticles were linked to dopamine, single-stranded DNA oligonucleotides with the sequence 5'cdTGG-TATATATATATATAT 3' (1) and double-stranded DNA with the sequence 5'cdTGGTATATATATATATAT 3' hybridized with 5' ATATATATATATATACCA (2) were spotted onto a glass plate in the presence of silver ions. The samples were illuminated with 100 W white light for 5 min. The brown color indicates metallic silver deposition following accumulation of photogenerated electrons on  $\text{TiO}_2$  nanoparticles as a result of extended charge separation.

of spin density on the pendant  $\text{CH}_2\text{-CH}_2\text{-NH}_2$  side chain of dopamine.<sup>13</sup> The delocalization of photogenerated holes to the pendant side chain suggests dopamine as a ligand of choice for linking nanoparticles to biomolecules, because it can act as a conduit of photogenerated charges and enables further extension of charge separation.

A variety of 16-base pair oligonucleotides terminated with carboxyl deoxythymidin-e (cdT) were attached to the pendant amino groups of dopamine and chemisorbed on the  $\text{TiO}_2$  surface. The EPR spectrum obtained after photoexcitation of single-stranded DNA/ $\text{TiO}_2$  composite (ss DNA/ $\text{TiO}_2$ ) at 10 K was identical to that obtained upon illumination of dopamine-modified  $\text{TiO}_2$  (Figure 3, top). This result indicates that in the single-stranded  $\text{TiO}_2$ /DNA nanocomposite charge separation at 10 K terminates at dopamine and never reaches DNA oligonucleotide. Subsequently,  $\text{TiO}_2$  attached oligonucleotides were hybridized with their complementary strands in order to create double-stranded DNA/ $\text{TiO}_2$  nanocomposites (ds DNA/ $\text{TiO}_2$ ). Following photoexcitation at 10 K, an EPR signal distinct from the EPR spectrum of dopamine-modified  $\text{TiO}_2$  was observed. This signal, obtained

with two different attached oligonucleotides, is a multiline spectrum with a total width of 100 G (Figure 3 top curve 2).

The EPR spectrum resembles that of radicals obtained for oxidized DNA at low temperature,<sup>27</sup> but does not duplicate the shapes of signals obtained following oxidative damage of the four nucleic bases that constitute DNA. The main features of the signal obtained upon illumination of  $\text{TiO}_2$ /DNA nanocomposite at 10 K could be reasonably simulated assuming hole trapping on cdT (Figure 4). The oxidation of cdT as a primary hole trapping site at 10 K is not expected, considering that thymidine itself should not be oxidized by photogenerated holes on  $\text{TiO}_2$ . Therefore, theoretical modeling of the redox properties of thymidine derivatives in gas phase and in aqueous solution was carried out.<sup>28</sup> The computational results indicate that the addition of a carboxyl group to thymine at position 5 (replacing a methyl group) lowers the adiabatic ionization potential of thymine in aqueous solution by 0.08 eV (Figure 5). Furthermore, it was found that condensation of carboxyl thymine (cT) with an amino group into a peptide bond (ncT) leads to further

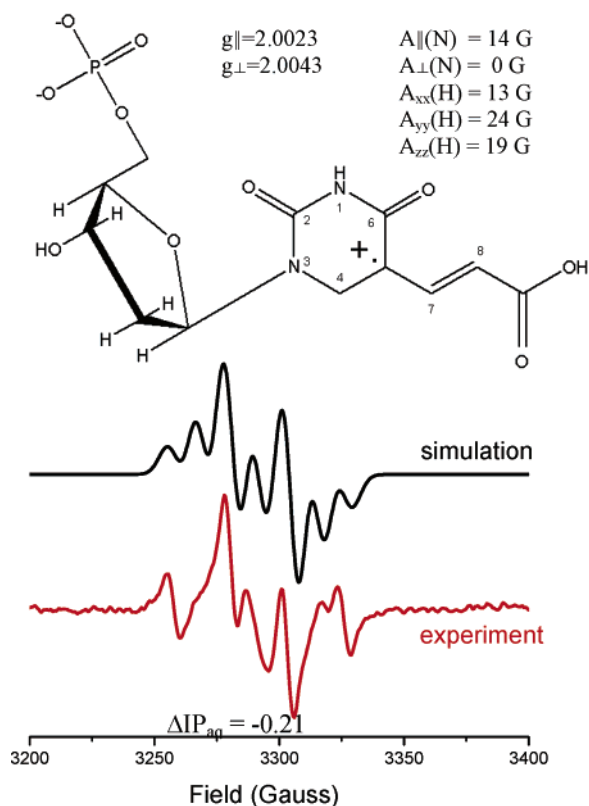


**Figure 4.** Comparison of experimental and simulated spectra of oxidized carboxyl deoxythymidine radical (cdT). The spectra were simulated using “Simfonia” simulation program (Bruker Instruments Inc.) using the parameters indicated in the figure. The parameters used to simulate the cdT cation radical were consistent with the hyperfine interactions of one proton from the CH group at the position 7 and two nitrogen atoms of the pyrimidine ring. The anisotropic g-tensors and hyperfine couplings are consistent with the parameters used in previous simulations of frozen solutions containing cation radicals of pyrimidines.<sup>22</sup>

lowering of the ionization potential by an additional 0.12 eV. Hydrogen bonding following base pairing of ncT with adenine introduces additional changes in the ionization potential, resulting in further reduction of the ionization potential of the ncT•••A pair by 0.13 eV. We believe that this last step of base pairing is responsible for our observation that the most efficient electron transfer occurs in double-stranded oligonucleotides attached to TiO<sub>2</sub>. As the oxidation potential of ncT decreases upon base pairing, ncT•••A does not impose a barrier for hole hopping and the oxidation of double-stranded DNA oligonucleotides becomes efficient (Figure 1a). On the other hand, when single-stranded DNA oligonucleotides are linked to TiO<sub>2</sub> nanoparticles, photogenerated holes do not have enough driving force to overcome the barrier imposed by cdT and photogenerated holes, localized at dopamine, recombine with electrons on neighboring TiO<sub>2</sub> nanoparticle (Figure 1b).

We have also investigated the charge separation in these systems at room temperature by using silver reduction as a reporter of the number of electron-transfer events (Figure 3b). Silver ions have a positive deposition potential, and when excess electrons are present in TiO<sub>2</sub> nanoparticles, silver ions act as acceptors for these photogenerated electrons

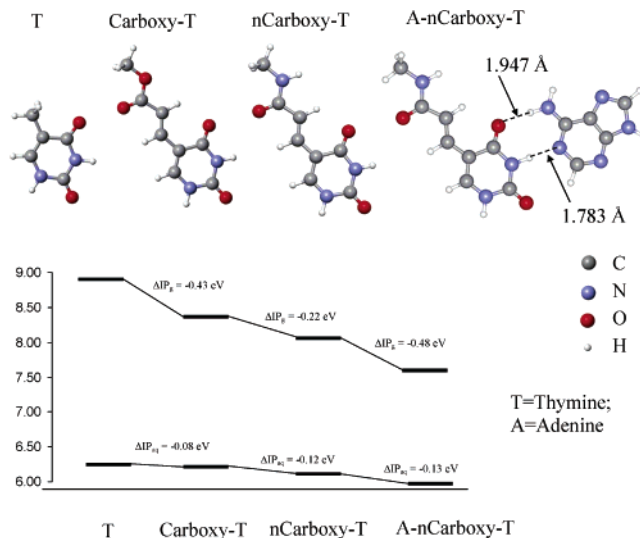


**Figure 5.** Theoretical modeling of the structure and ionization potentials of thymine, carboxyl thymine and carboxyl thymine-adenine pair. The structures and ionization potentials of thymine (T) and carboxyl thymine (CT) and CT•••A pair in the gas phase and aqueous solution were calculated<sup>26</sup> at the B3LYP/6-31+G\*\*//B3LYP/6-31G\*\* level of theory, including zero-point energy correction. The solvation was treated using the self-consistent reaction field and polarized continuum model. Solvation reduces ionization potentials. Functionalization of thymine by the amino-modified carboxyl group improves its electron-donating properties and the choice of linker strongly influences properties of the base pair.

(A, Figure 1) and are reduced to their metallic form. As in the photographic process, the amount of the silver deposited on the TiO<sub>2</sub> particles, and subsequent color intensity, is proportional to the number of electrons that have survived charge separation. In this manner the amount of deposited silver is proportional to the lifetime of charge-separated state. Hence, silver ions were added into the solution of DNA/TiO<sub>2</sub> nanocomposites and the sample was dried on a glass plate. Illumination of the glass plate resulted in significant silver deposition in the areas where dsDNA/TiO<sub>2</sub> nanocomposites were spotted, indicating that hybridized DNA molecules act as efficient electron donors that allow photocatalytic deposition of metallic silver on TiO<sub>2</sub> nanoparticles (Figure 3 bottom, spot 2). Deposition of metallic silver in ssDNA/TiO<sub>2</sub> nanocomposites was much less intense, suggesting the existence of the barrier for extended charge separation, in agreement with the low-temperature EPR results (Figure 3 bottom, spot 1). This small amount of deposited silver may be the result of thermal mobility of single-stranded DNA at room temperature.<sup>29</sup> It should be noted that deposition of metallic silver was not significant for samples of TiO<sub>2</sub> linked only to dopamine under the same conditions (Figure 3 bottom), or in a system in which dsDNA was linked through a polythymine linker (12T). Additionally, when one or two mismatches (GT) were introduced into the sequence of dsDNA, deposition of silver was reduced (Figure 6a). Addition of GT mismatches prevents guanine bases from participating in hole hopping within DNA. The decrease in the efficiency of silver deposition followed long-range electron-transfer correlation (efficiency  $\propto N^{-\eta}$ ,  $\eta$  in these

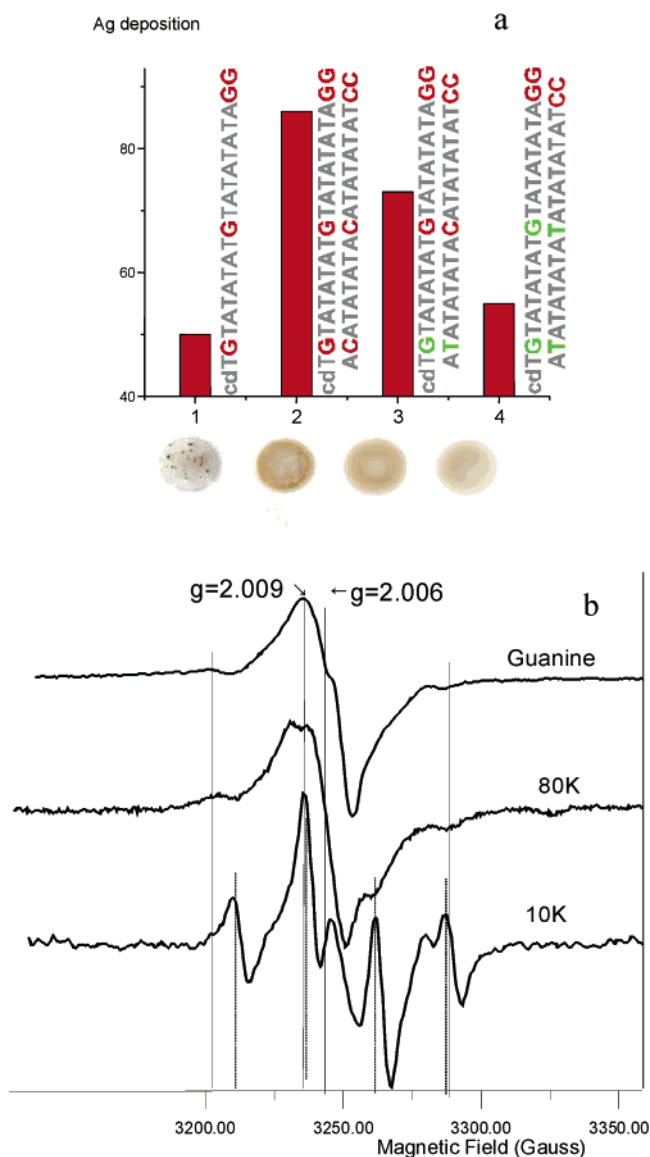


**Figure 6.** Sequential charge separation in  $\text{TiO}_2$ /oligonucleotide nanocomposites studied by (a) photoreduction of silver ions under ambient conditions.  $\text{TiO}_2$  nanoparticles were linked to dopamine, single-stranded DNA oligonucleotides with the sequence 5'cdTG-TATATATGTATATATAGG 3' (1) fully matched double-stranded (ds) DNA with the sequence 5'cdTG-TATATATGTATATATAGG 3' hybridized with 5' CCTATATATAACATATATACA 3' (2), dsDNA with one GT mismatch (3), and dsDNA with two GT mismatches (4). Mismatches are indicated in the figure in green color. The samples were illuminated with 100 W white light for 1 min. The brown color indicates metallic silver deposition following accumulation of photogenerated electrons on  $\text{TiO}_2$  nanoparticles as a result of extended charge separation. (b) Monitoring temperature dependence of EPR spectra. The multiline spectrum observed at 10 K (bottom) as cdT radical transforms upon annealing at 80 K into a broad signal at  $g = 2.006$  (middle). This spectrum is distinctly different from the spectrum obtained upon oxidation of dopamine under the same experimental conditions but reproduces the feature obtained upon oxidation of guanine with OH radicals under the same conditions (top).

experiments was 0.5).<sup>30,31</sup> The experiments were performed in three different double strands, where the number of electron-transfer steps over the distance of 66 Å was varied from 3 to 1.

The sequential steps in the hole trapping process were studied through the temperature dependence of the EPR signal. Warming of the sample induces a change in the EPR spectrum indicative of further charge hopping. Upon annealing at 80 K, the EPR signal collapses into a signal with a very weakly resolved hyperfine structure and weak satellite lines (Figure 6b). The EPR spectrum of the guanosine radical cation obtained by reaction with radiolytically generated OH radicals matches the 80 K spectrum. This result indicates that sequential hole transfer to guanine in DNA follows the initial charge separation between the end-group cdT radical and  $\text{TiO}_2$  nanoparticle. In this manner, the absorption of light by the DNA/ $\text{TiO}_2$  system is followed by sequential electron transfer of photogenerated electrons through a series of electron trapping sites. Therefore, illumination of  $\text{TiO}_2$ /DNA composites results in a light conversion event in which light energy is transduced into separated electrons and positive holes, stabilized by physical separation. It should be noted that in polythymidine-bridged dsDNA attached to  $\text{TiO}_2$  particles, extended charge separation, monitored by silver deposition, was not observed. In this case charge never reaches the DNA oligonucleotides, suggesting that an activation barrier controls the electron-transfer processes in the hybrid systems, similar to the case of DNA alone.<sup>29,32</sup> Furthermore, linking of DNA through thymidine bridges prevents the photoinduced redox chemistry that occurs in hybrid  $\text{TiO}_2$ /oligonucleotide triads. Therefore, controlling the sequence of the bridging groups of DNA oligonucleotides allows for the control of the electron transfer process across the interface. This approach provides the opportunity for linking multiple DNA oligonucleotides to nanocrystalline particles, some having redox functions and others having only recognition functions capable of continuing naturally designed biological activities upon illumination. In this manner one can envision multifunctional triads carrying out simultaneously a variety of functions involved in manipulation of genetic materials.<sup>7</sup>

In summary, we have shown that binding of double-stranded oligonucleotides to photoactive metal oxide particles results in a photoelectrochemical system capable of extended charge pair separation. These systems (triads) may form a basis for designing sensors for DNA hybridization. The same method could be used for the detection of DNA binding polypeptides due to the change of redox properties of DNA after binding to proteins. This approach creates an opportunity for a new family of site-specific biomolecule electronic sensors and/or electronically tunable site-specific metal oxide catalysts. Multiple electron transfers in this system may also result in cleavage of DNA, forming a basis for in vivo intracellular devices capable of genetic manipulation and genetic detection.<sup>7</sup> Full realization of these potential implementations requires detailed understanding of charge separation in these composite materials. Future studies will address in detail the effects of length, sequence, and the DNA structure (mismatches) on charge accumulation and consequently signal transduction.

**Acknowledgment.** This work was supported by the U.S. DOE, Office of BES, Division of Chemical Sciences, under

contract W-31-109-Eng-38. J.L. and N.F.S. were supported by University of Chicago-Argonne National Laboratory Consortium for Nanoscience Research. The authors acknowledge the insights gained from discussions with D. Roitman and P. Kuekes. T.R. and N.F.S. thank S. Ranc for assistance with AFM measurements.

## References

- (1) Storhoff, J. J.; Mirkin, C. A. *Chem. Rev.* **1999**, *99*, 1849.
- (2) Pease, A. C.; Solas, D.; Sullivan, E. J.; Cronin, M. T.; Holmes, C. P.; Fodor, S. P. A. *Proc. Natl. Acad. Sci. U.S.A.* **1994**, *91*, 5022.
- (3) Gerion, D.; Chen, F.; Kannan, B.; Fu, A.; Park, W. J.; Chen, D. J.; Majumdar, A.; Alivisatos, A. P. *Anal. Chem.* **2003**, *75*, 4766.
- (4) Taton, T. A.; Mirkin, C. A.; Letsinger, R. L. *Science* **2000**, *289*, 1757.
- (5) Hodneland, C. D.; Mrksich, M. *J. Am. Chem. Soc.* **2000**, *122*, 4235.
- (6) Patolsky, F.; Lichtenstein, A.; Willner, I. *J. Am. Chem. Soc.* **2000**, *122*, 418.
- (7) Paunesku, T.; et al. *Nature Materials* **2003**, *2*, 343.
- (8) Moore, T. A.; Gust, D.; Mathis, P.; Mialocq, J. C.; Chachaty, C.; Bensasson, L. *Nature* **1984**, *307*, 630.
- (9) Wasielewski, M. R.; Niemczyk, M. P.; Johnson, D. G.; Svec, W. A.; Minsek, D. W. *Tetrahedron* **1989**, *45*, 4785.
- (10) Serpone, N.; Pelizzetti, E.; Eds. *Photocatalysis*; Wiley: New York, 1989.
- (11) Rajh, T.; Chen, L. X.; Lukas, K.; Liu, T.; Thurnauer, M. C.; Tiede, D. M. *J. Phys. Chem. B* **2002**, *106*, 10543.
- (12) Surface modification of TiO<sub>2</sub> nanoparticles was found to result in a red shift of the TiO<sub>2</sub> absorption compared to unmodified nanocrystallites. The optical shift correlates with the dipole moment of the Ti-ligand complexes at the surface and decreases with the ligand size. It was found that dihydroxycyclobutenedione shifts the optical absorption and effective band gap of TiO<sub>2</sub> by 0.8 eV, ascorbic acid by 1.2 eV, dopamine by 1.9 eV, *tert*-butyl catechol by 2.0 eV, and alizarine by 1.4 eV. Upon surface modification, the position of the Fermi level and concomitantly the conduction band of TiO<sub>2</sub> (intrinsically n-type) are slightly altered by 0.1 eV, thus the reducing properties are not changed significantly (Dimitrijevic; et al. *J. Phys. Chem. B* **2003**, *107*, 7368). Consequently, the main effect of surface modification is a change of the oxidative properties of ligand-modified nanoparticles, and this can be tuned with different ligands.
- (13) Rajh, T.; Poluektov, O.; Dubinski, A. A.; Wiederrecht, G.; Thurnauer, M. C.; Trifunac, A. D. *Chem. Phys. Lett.* **2001**, *344*, 31.
- (14) Steenken, S.; Jovanovic, S. V. *J. Am. Chem. Soc.* **1997**, *119*, 617.
- (15) Wamer, W. G.; Yin, J. J.; Wei, R. R. *Free Radical Biol. Med.* **1997**, *23*, 851.
- (16) Dunford, R.; Salinaro, A.; Cai, L. Z.; Serpone, N.; Horikoshi, S.; Hidaka, H.; Knowland, J. *FEBS Lett.* **1997**, *418*, 87.
- (17) Micic, O. I.; Rajh, T.; Comor, M. V. In *Electrochemistry in Colloids and Dispersions*; Mackey, R. A., Texter, J., Eds.; VCH: New York, 1992; p. 457.
- (18) Colloidal TiO<sub>2</sub> was prepared by dropwise addition of titanium(IV) tetrachloride to water cooled to 4° The temperature and component mixing of reactants were controlled by an apparatus developed for automatic colloid preparation.<sup>11</sup> TiO<sub>2</sub> colloids were diluted to 0.015 M and mixed with 100 μL of glycidil isopropyl ether (which then coats the TiO<sub>2</sub> nanoparticles and helps preserve the biofunction of the oligonucleotides, preventing undesirable reactions of hydroxyl groups at the TiO<sub>2</sub> surface with phosphodiester groups of the oligonucleotides). With vigorous mixing, 0.2 M LiOH was rapidly injected into the TiO<sub>2</sub> solution until a pH of 9.5 was reached. TiO<sub>2</sub> nanoparticles of 45 Å (about 1500 TiO<sub>2</sub> molecules per particle) prepared in this way were dialyzed against 10 mM NaH<sub>2</sub>PO<sub>4</sub> until pH 6.5 was obtained. The size of the TiO<sub>2</sub> nanoparticles was determined by transmission electron microscopy. (All the chemicals were reagent grade (Aldrich or Baker) and used without further purification.) DNA oligonucleotides were synthesized with the 5' terminal carboxyl group (Operon Co) and kept as a 10 μM solution in 10–40 mM phosphate buffer at pH 6.5. A condensation reaction through intermediate *N*-hydroxy-succinimide ester was used to bind the carboxyl group of the oligonucleotide to the amino group of dopamine by an amide bond. In the first step, the DNA terminal carboxyl group is bound to *O*-*N*-succinimidyl-*N*NNN-tetramethyluronium tetrafluoroborate in the presence of *N,N*-diisopropylethylamine in DMF. In the second step, the succinimidyl group is replaced with dopamine through its terminal amino group in the presence of dioxane. This solution was thoroughly dialyzed against water to remove free dopamine unbound to oligonucleotides. In the final step, dopamine end-labeled oligonucleotides are bound to TiO<sub>2</sub> particles modified by glycidil isopropyl ether. When dopamine (free or bound to oligonucleotides) is added into TiO<sub>2</sub> colloidal solutions at 8 > pH > 2.5, the immediate development of a red color indicates instantaneous formation of a charge-transfer complex between dopamine and TiO<sub>2</sub>. The dopamine/TiO<sub>2</sub> complex is extremely stable and cannot be easily removed by dialysis; bidentate binding stabilizes the complex because of the chelating effect. Stability of the complex is greater than the stability of the complex between TiO<sub>2</sub> glycidil isopropyl ether and therefore replaces it from the surface.<sup>11</sup> The calibration curve for the number of dopamines adsorbed per TiO<sub>2</sub> particle was obtained by measuring absorption of TiO<sub>2</sub>/DA complex at different wavelengths. The extinction coefficient of the absorption of dopamine/TiO<sub>2</sub> complex at 440 nm is 3.3 × 10<sup>3</sup> M<sup>-1</sup> cm<sup>-1</sup>, at 520 nm is 1.1 × 10<sup>3</sup> M<sup>-1</sup> cm<sup>-1</sup>, and at 570 nm is 1.0 × 10<sup>3</sup> M<sup>-1</sup> cm<sup>-1</sup>. The concentration of TiO<sub>2</sub>/DA/DNA complex formed after linking was determined from a calibration curve. The stability of dopamine-modified TiO<sub>2</sub> colloids is preserved after exposure to thousands of 10 mJ laser pulses and daylight for several years. Oligonucleotides modified nanoparticles are stable for up to one month when stored in the refrigerator. The particle concentration of the nanocomposites was approximately 15 μM.
- (19) Bonacheva, M. Schibler, L.; Lincon, P.; Vogel, H.; Akerman, B. *Langmuir* **1999**, *15*, 4317.
- (20) Banwarth, W.; Schmidt, D.; Stallard, R. L.; Hornung, C.; Knorr, R.; Muller, F. *Helv. Chim. Acta* **1988**, *71*, 2085.
- (21) Arkin, M. R.; Stemp, E. D. A.; Holmlin, R. E.; Barton, J. K.; Hormann, A.; Olson, E. J. C.; Barbara, P. F. *Science* **1996**, *273*, 475.
- (22) Lewis, F. D.; Wu, T.; Zhang, Y.; Letsinger, R. L.; Greenfield, S. R.; Wasielewski, M. R. *Science* **1997**, *277*, 673.
- (23) Sevilla, M. D.; Suryanarayana, D.; Morehouse, K. M. *J. Phys. Chem.* **1981**, *85*, 1027.
- (24) Bernhard, E. A. *Adv. Radiat. Biol.* **1981**, *9*, 199.
- (25) Radical species involved in the initial charge separation of the charge-transfer complex of TiO<sub>2</sub> nanoparticles covered with a monolayer of dopamine were investigated in detail previously.<sup>11,13</sup> However, in the experiments described in the text, only 2–3 dopamine molecules were linked to the TiO<sub>2</sub> nanoparticles as conduits to DNA oligonucleotides. Therefore, the observed spectra are weak and broad (due to the absence of ordering of dopamine molecules compared to monolayer coverage). The EPR signal attributed to trapped electrons appears weaker compared to the dopamine signal at low dopamine coverage because of axial anisotropy of titanium signal in the anatase environment in which the signal is spread over perpendicular and parallel components.
- (26) Rajh, T.; Nedeljkovic, J.; Chen, L. X.; Poluektov, O.; Thurnauer, M. C. *J. Phys. Chem. B* **1999**, *103*, 3515.
- (27) Frisch, M. J.; Trucks, G. W.; Schlegel, H. B.; Scuseria, G. E.; Robb, M. A.; Cheeseman, J. R.; Zakrzewski, V. G.; Montgomery, J. A., Jr.; Stratmann, R. E.; Burant, J. C.; Dapprich, S.; Millam, J. M.; Daniels, A. D.; Kudin, K. N.; Strain, M. C.; Farkas, O.; Tomasi, J.; Barone, V.; Cossi, M.; Cammi, R.; Mennucci, B.; Pomelli, C.; Adamo, C.; Clifford, S.; Ochterski, J.; Petersson, G. A.; Ayala, P. Y.; Cui, Q.; Morokuma, K.; Malick, D. K.; Rabuck, A. D.; Raghavachari, K.; Foresman, J. B.; Cioslowski, J.; Ortiz, J. V.; Stefanov, B. B.; Liu, G.; Liashenko, A.; Piskorz, P.; Komaromi, I.; Gomperts, R.; Martin, R. L.; Fox, D. J.; Keith, T.; Al-Laham, M. A.; Peng, C. Y.; Nanayakkara, A.; Gonzalez, C.; Challacombe, M.; Gill, P. M. W.; Johnson, B. G.; Chen, W.; Wong, M. W.; Andres, J. L.; Head-Gordon, M.; Replegle, E. S.; Pople, J. A. *Gaussian 98*, revisions A.7 and A.11.4; Gaussian, Inc.: Pittsburgh, PA, 1998.
- (28) Vega-Arroyo, M.; LeBreton, P. R.; Rajh, T.; Zapol, P.; Curtiss, L. A. *Chem. Phys. Lett.* **2003**, *380*, 54.
- (29) Giese, B. *Acc. Chem. Res.* **2000**, *33*, 631.
- (30) Jortner, J.; Bixon, M.; Langenbacher, T.; Michel-Beyerle, M. E. *Proc. Natl. Acad. Sci. U.S.A.* **1998**, *95*, 12759.
- (31) Lewis, F. D.; Letsinger, R. L.; Wasielewski, M. R. *Acc. Chem. Res.* **2001**, *34*, 159.
- (32) Henderson, P. T.; Jones, D.; Hampikian, G.; Kan, Y.; Schuster, G. B. *Proc. Natl. Acad. Sci. U.S.A.* **1999**, *96*, 8353.

NL049684P